UDC 539.1.074
SCOPUS CODE 3101
https://doi.org/10.36073/1512-0996-2026-2-175-191

LED-Based Calibration System for SiPM Radiation Damage Studies

Aleks Mestvirishvili Georgian technical university institute of quantum physics and engineering technologies, senior research scientist, Georgia
E-mail: alexi.mestvirishvili@cern.ch

Yuri Bagaturia Georgian technical university institute of quantum physics and engineering technologies, senior research scientist, Georgia
E-mail: Iuri.bafaturia@cern.ch

Abesalom Iashvili Georgian technical university institute of quantum physics and engineering technologies, senior research scientist, Georgia
E-mail: iashviliab@yahoo.com

Davit Lomidze Georgian technical university institute of quantum physics and engineering technologies, senior research scientist, Georgia
E-mail: David.lomidze@cern.ch

Irakli Lomidze Georgian technical university institute of quantum physics and engineering technologies, senior research scientist, Georgia
E-mail: Irakli.lomidze@cern.ch

Tengiz Toriashvili Georgian technical university institute of quantum physics and engineering technologies, senior research scientist, Georgia
E-mail: Tengizi.toriashvili@cern.ch

Zviad Tsamalaidze Georgian technical university institute of quantum physics and engineering technologies, senior research scientist, Georgia
E-mail: ZviadiTsamalaidze@cern.ch

Reviewers:
I. Minashvili, joint institute for nuclear reaserch, senior reaserch Dubna fellow
E-mail: Irakli.minashvili@cern.ch
D. Chokheli, Georgian Technical University joint institute for nuclear reaserch, senior reaserch fellow
E-mail: dchokhel@cern.ch

Abstract.

A compact LED-based calibration system has been developed for the characterization of silicon photo-multipliers (SiPMs). Such calibration stations are essential for accurate gain determination, breakdown-voltage monitoring, and long-term stability studies in modern pho- todetector applications [1,2]. The system combines a DAC-controlled switching power supply for LED biasing with an external fast pulser that generates

short, programmable electrical pulses. This note describes the main building blocks of the system and their role in producing low-intensity, well-defined optical signals suitable for single-photon and few-photon measurements.

This research [Grant number FR-22-985] has been supported by Shota Rustaveli National Science Foundation of Georgia (SRNSFG).

Keywords: Calibration Station; Pulses; Poto-detection systems; Silicon phtorutilliers.

Introduction

The LT3482 integrates a high-voltage switch, internal charge pump, and current monitor amplifier, enabling efficient step-up con- version with minimal external components. Each channel includes a 6.8 μH inductor, high-voltage rectification and filtering capacitors, and a resistive feedback network to define the output voltage.

Main Part

High-Voltage Power Supply System Based on LT3482

A compact multi-channel high-voltage power supply (HVPS) was developed to bias silicon photomultipliers (SiPMs) and other solid-state photon sensors requiring stable and adjustable bias voltages up to approximately 100 V. Each channel is based on the LT3482 monolithic photodiode bias IC [3], as illustrated in the schematic in Fig. 2.[1]

Design Concept: Switching frequency is set using a resistor on the FSET pin, allowing optimization between ripple performance and efficiency.

1Schematic reference: LT3482 power supply channels.

1.1 Digital Voltage Control

Output voltage is digitally programmed via a four-channel precision DAC (Texas Instruments DAC60504 [4]), which biases the FB pin of each LT3482. This architecture allows controlled setting of the SiPM bias voltage in software, enabling automated calibration routines. For laboratory operation, fine control over the voltage range ensures operation slightly above the SiPM breakdown voltage.

1.2 Current and Voltage Monitoring

Each bias channel includes digital instrumentation to ensure operational stability and prevent damage in case of abnormal current increases. The LT3482 features a MON pin that provides a voltage proportional to the output current. This signal is routed to a Texas Instruments INA228 preci- sion current and power monitor [5], which measures the MON pin voltage using its differential inputs and digitizes the resulting current information over an I^2C interface.

In addition, the output voltage is monitored via a high-voltage OPA452 operational amplifier [6], which provides a protected, low-impedance V_{BUS} sense signal for the INA228. This combination enables simultaneous readout of both SiPM current and bias voltage, supporting accurate gain calibration and breakdown-voltage tracking.

[1]Schematic reference: LT3482 power supply channels.

LT3482 Bias and Monitoring Block Diagram.

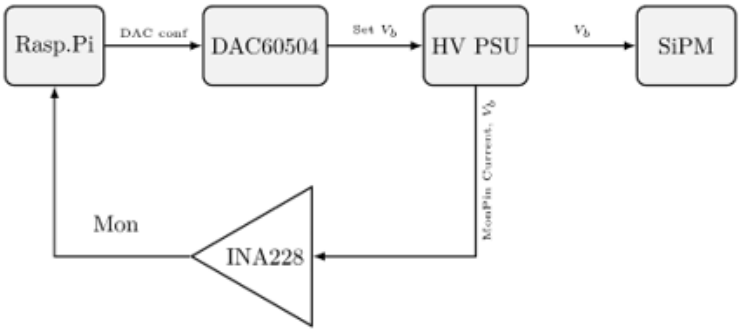

Figure 1: Block diagram of SiPM bias and voltage monitoring.

1.3 Output Filtering and Interface

Each bias output channel is equipped with a LEMO coaxial connector for external sensor connection. The output includes additional RC filtering to suppress switching transients and ground-bounce noise. A dedicated shutdown control pin allows each channel to be individually disabled under software control for safe configuration and during fault recovery.

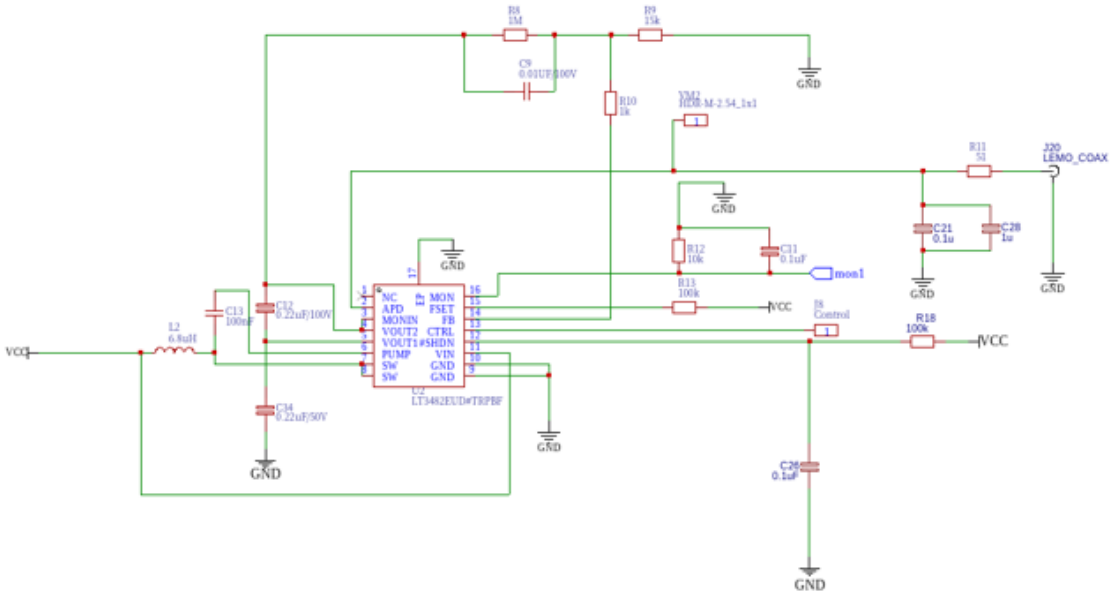

Figure 2: Schematic of a single LT3482 HV power supply channel

Prior to PCB fabrication, each channel topology was validated in LT- spice [12]. Startup transient behavior, output voltage regulation, and ripple characteristics were analyzed over the full operating voltage range and expected SiPM load currents. Simulation results guided passive component selection including the inductor value, compensation capacitors, and output filtering.

1.4 LTspice Simulation and Validation

Figures 3–5 summarize LTspice and laboratory test results characterizing voltage linearity, ripple stability, and transient behavior of the LT3482-based high-voltage supply.

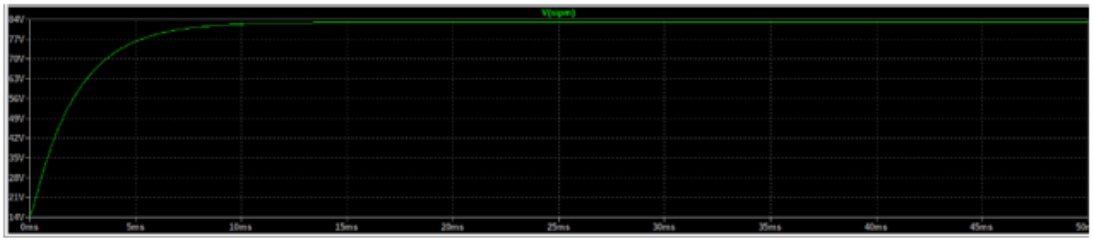

Figure 3: Simulated startup response of the LT3482 SiPM bias channel. The output reaches stable voltage in approximately 20 ms with clean settling and no overshoot.

Figure 4 shows zoomed-in view of the SiPM bias output in steady-state operation. Output ripple remains in the range of only a few tens of microvolts at approximately 83 V, confirming very low-noise performance. This confirms that switching artifacts are well suppressed through filtering and proper PCB grounding, making the supply suitable for low-noise photon detector biasing.

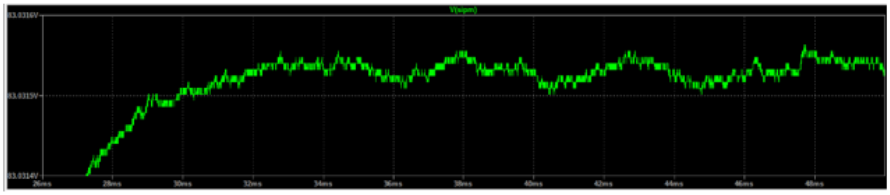

Figure 4: Simulated steady-state output ripple of the SiPM bias supply. Ripple amplitude remains below a few 10s of μV at ≈83 V

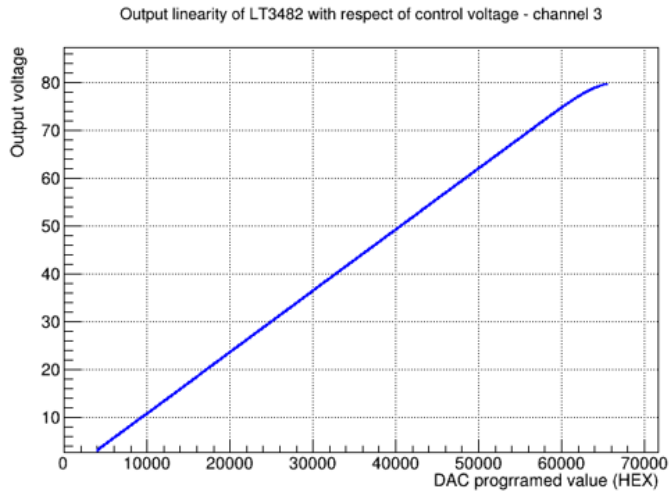

Figure 5: Output voltage linearity of an LT3482-based HV channel vs. DAC programmed value. The bias voltage shows monotonic and nearly linear control over the full operating range.

This measurement demonstrates that the DAC-controlled feedback network provides stable and predictable voltage programming with no discontinuities or hysteresis effects.

1.5 Scalability and System Integration

The current implementation supports four independent HV bias channels. Due to the modular architecture, extending the design to eight or more channels requires only:

replication of the LT3482 block and passive components,

• and additional DAC + sensing interfaces.

The system integrates seamlessly with the single-board computer (SBC) control infrastructure already used for LED pulsing, enabling unified software management of:

• SiPM bias voltage,

• LED pulse amplitude and timing,

• real-time current and voltage monitoring.

This flexible and digitally controlled HVPS makes the system suitable for extensive SiPM characterization, gain calibration, and long-term stability studies.

2 LED Calibration Light Source

To generate a controlled low-intensity optical signal for SiPM calibration, a blue LED is biased using a programmable DC power supply based on the LM2596 adjustable switching regulator [7]. The regulator's output voltage is dynamically controlled by an external 12-bit MCP4725 digital-to-analog converter (DAC) [8], allowing precise adjustment of the average LED light level over a wide dynamic range.

On top of this continuously adjustable DC bias, fast optical pulses are introduced by briefly modifying the LED current. A low-power N-channel MOSFET (BSS123) is connected in the LED cathode path and is driven by the fast pulser described in Section 3. When the MOSFET is switched on, the LED current is slightly increased, producing very weak but well-defined light pulses suitable for single-photon response studies.

The LED is connected externally via a header, which also allows flexible installation of an additional series resistor. This optional resistor enables fine control of the modulation depth by introducing a small difference between the LED current during pulsed and non-pulsed states.

3 Fast LED Pulser

A dedicated fast pulser circuit was developed to generate short electrical pulses for LED excitation in calibration measurements. The pulser consists of a programmable delay line, a high-speed comparator, and fast CMOS logic for pulse shaping and timing control. Configuration and operation of the pulser are performed by the SBC via its GPIO pins.

3.1 Control and Timing Concept

Several GPIO pins from the SBC are connected directly to the control inputs of a DS1023 programmable delay line [9]. One of the GPIO lines is used as a digital trigger signal. The DS1023 generates a delayed version of this trigger according to a programmable control code written by the SBC. In this way, the effective delay—and hence the outgoing pulse width—is set entirely in software.

Both the original trigger and the delayed signal are then processed by a dual high-speed comparator (LT1720 [10]). The comparator provides fast edge sharpening and clean logic transitions, which are important for generating well defined, short pulses at the output. Comparator outputs are subsequently combined by a quad 2-input AND gate (SN74AHC08 [11]). Only the time interval where both comparator

outputs are simultaneously high defines the final electrical pulse, making the pulse width directly proportional to the programmed delay difference.

Additional AC-coupling and trimming elements are included at the input stage in order to prevent accidental triggering and to allow fine threshold adjustments. A separate header connector provides an option for external triggering if needed.

Figure ?? shows the functional block diagram of the external fast pulser. The SBC provides both the trigger signal and the configuration signals to the delay line. The delay line, comparator, and AND logic form a compact chain that converts the trigger into a short, programmable-width output pulse.

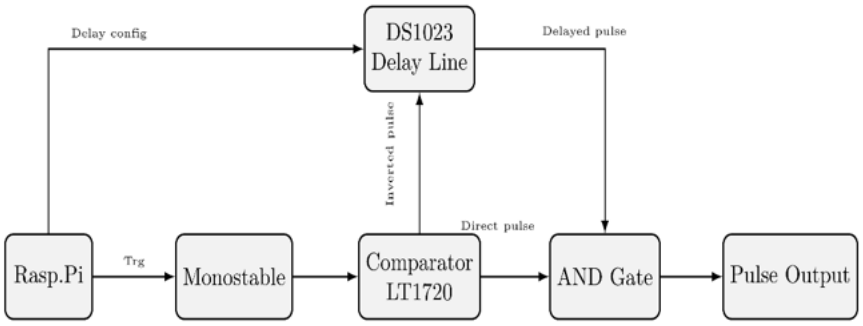

Figure 6: Block diagram of the fast pulser logic. The SBC drives a monostable that feeds the LT1720 comparator. The comparator generates direct and inverted pulses: one path goes directly to the AND gate, while the inverted pulse is routed through the DS1023 delay line before entering the second AND input. The resulting AND output is a short pulse with width defined by the programmed delay.

3.2 Pulse Width Range and Rise Time Performance

The pulser can generate a wide range of pulse widths depending on the programmed delay. As shown in Fig. 7, the shortest achievable pulse is approximately 10 ns wide (10 ns/div). The longest programmable pulse width is demonstrated in Fig. 8, where the delay line is configured to its maximum range (200 ns/div).

Figure 9 shows the leading edge transition, exhibiting a rise time below 4 ns (2 ns/div). The rise time is extracted using the standard 10% → 90% definition, with linear interpolation between digitizer samples to achieve subnanosecond accuracy. This confirms the pulser performance is sufficient for precise synchronization of single-photoelectron waveforms from SiPMs.

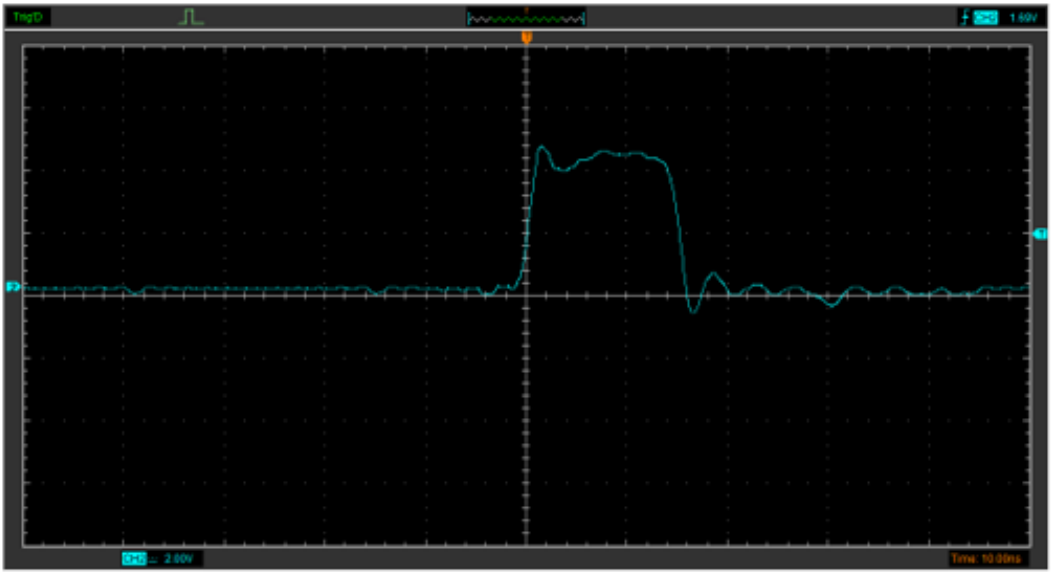

Figure 7: Shortest LED excitation pulse generated by the fast pulser. izontal scale: 10 ns/div.

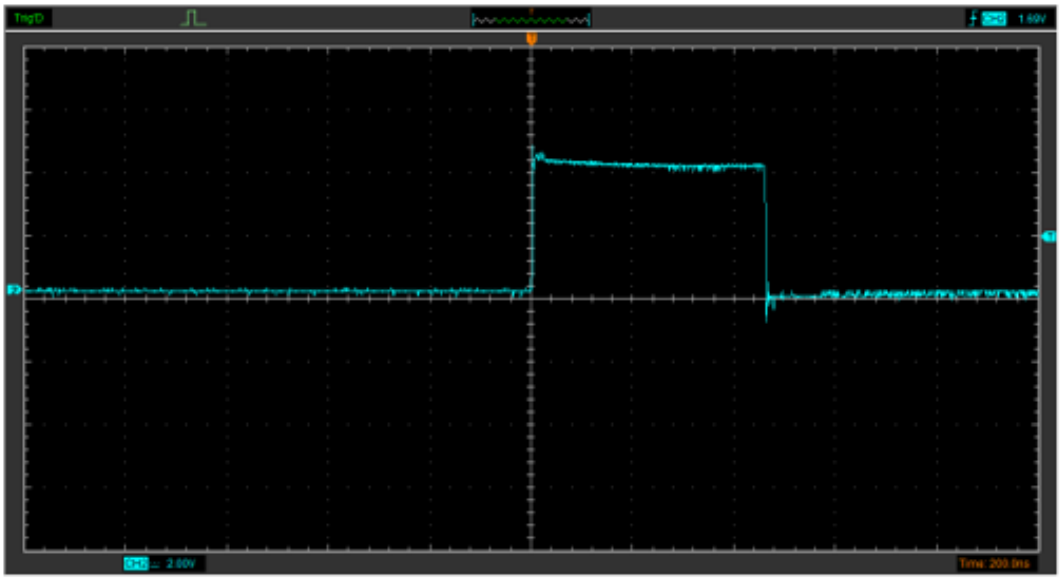

Figure 8: Maximum pulse width programmed via the delay line. scale: 200 ns/div.

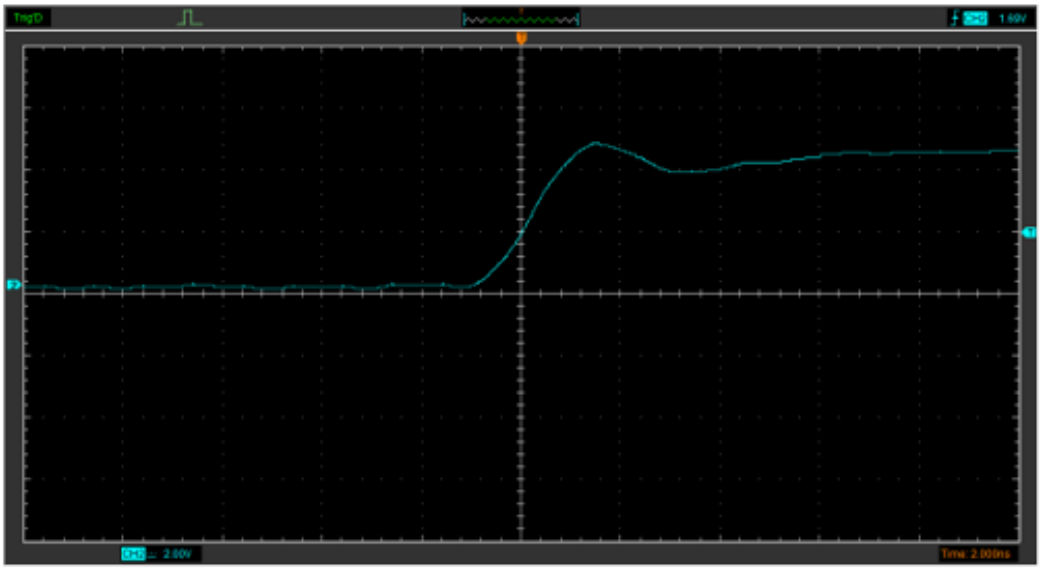

Figure 9: Rising edge performance of the pulser output. The measured rise time is < 4 ns using the 10% – 90% method. Horizontal scale: 2 ns/div.

SiPM Temperature Monitoring and Bias Compensation

Silicon photomultipliers exhibit a strong dependence of breakdown voltage on temperature. To maintain stable gain, the SiPM bias voltage must be adjusted in synchrony with temperature variations. Therefore, continuous temperature monitoring and real-time voltage compensation are implemented in the system.

4.1 PT100 Temperature Sensing and Constant-Current Excitation

Each SiPM module incorporates a PT100 platinum resistance temperature detector mounted in close thermal contact with the device package. A four- wire Kelvin configuration is implemented to eliminate errors due to harness resistance and connector variability, ensuring that only the intrinsic PT100 resistance contributes to the measured value.

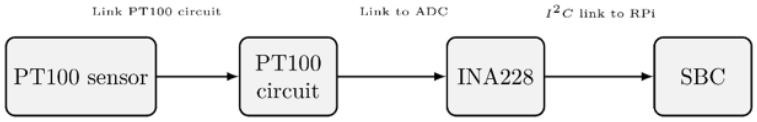

Figure 10: SiPM temperature measurment block diagram

To achieve high measurement accuracy and temperature stability, each PT100 is biased using a compact JFET-based constant-current source. A depletion-mode JFET (J310 [16]) configured with a self-bias feedback network maintains a nearly constant excitation current over supply voltagvariations and cable impedance changes. This approach ensures robust operation in distributed detector layouts.

The excitation current is set to 1.000 mA and verified during commis- sioning using a precision digital multimeter (Keithley 2000 [17]), providing better than microampere-level accuracy. At this current, the power dissi- pated in a 100 Ω PT100 is approximately 0.1 mW, resulting in less than 0.04°C self-heating based on typical sensor thermal resistance. This is neg- ligible compared to the temperature variations encountered in normal SiPM operation and therefore does not degrade bias-voltage compensation perfor- mance.

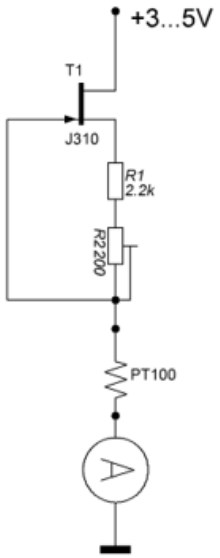

Figure 11: Constant-current excitation circuit used for PT100 biasing. The JFET (J310) with resistive self-feedback (R_1, R_2) stabilizes the sensing current at ≈ 1 mA, while the PT100 is read in a four-wire Kelvin configuration to ensure accurate temperature measurement.

4.2 Digitization Using INA228 Monitors

The PT100 resistance is measured using dedicated Texas Instruments INA228 digital current and power monitors. In this configuration, the INA228 acts as a precision ADC for the sensed resistance, converting it to temperature using a calibrated transfer function. An I^2C digital interface provides real- time temperature data to the main controller.

4.3 Automated Bias Stabilization

Temperature feedback enables the implementation of dynamic bias control. The system continuously evaluates whether the applied SiPM bias voltage remains consistent with the manufacturer-recommended operating condition at the measured temperature. If a deviation is detected, a watchdog control loop issues corrective commands to the high voltage supply, ensuring stable overvoltage $\Delta V = V_{bias} - V_{bd}(T)$.

This automated stabilization minimizes gain drift and supports long- duration measurements with constant photodetector performance. The approach is particularly beneficial in environmental conditions with slow thermal fluctuations or during characterization runs involving significant detec- tor self-heating.

5 Test with SiPM

5.1 Data Acquisition System

The SiPM output signals are digitized using a CAEN V1720 waveform acqui- sition module [14], providing

12-bit ADC resolution and a sampling rate of 250 MS⁄s. The module is operated in single-channel mode during the characterization measurements, with the input signals passed directly through the SiPM front-end network without additional shaping.

For remote operation and data readout, the V1720 is connected to the control computer (SBC) through a CAEN USB-to-Optical A4818 communication link [15]. This configuration ensures electrical isolation, immunity to electromagnetic interference, and reliable high-bandwidth data transfer from the detector environment to the processing unit.

The acquisition trigger is provided by the auxiliary output of the fast LED pulser, ensuring synchronous capture of SiPM waveforms with respect to the optical excitation pulses. This timing structure allows precise recon- struction of single-photoelectron charge spectra and enables detailed stabil- ity studies of the SiPM gain as a function of bias voltage and temperature.

5.2 Monitor-Pin Characterization with a Constant Load

Before connecting SiPMs, the high-voltage supply and monitor circuitry were evaluated using a resistive load to quantify the response of the LT3482 monitor pin (MON). A precision resistor of R = 4.3 MΩ was connected to the output, and the supply voltage was scanned from 25 V to 75 V. For each voltage point, two currents were determined: (i) the current inferred from the monitor pin, I_{MON}, multiplied by the nominal factor of five specified in the LT3482 datasheet, and (ii) the current expected from Ohm's law, $I = V_{out}/R$.

Across the full measurement range, the monitor-derived current agrees with the expected resistive current within experimental uncertainties, con- firming the linearity and accuracy of the MON pin. This validates the use of

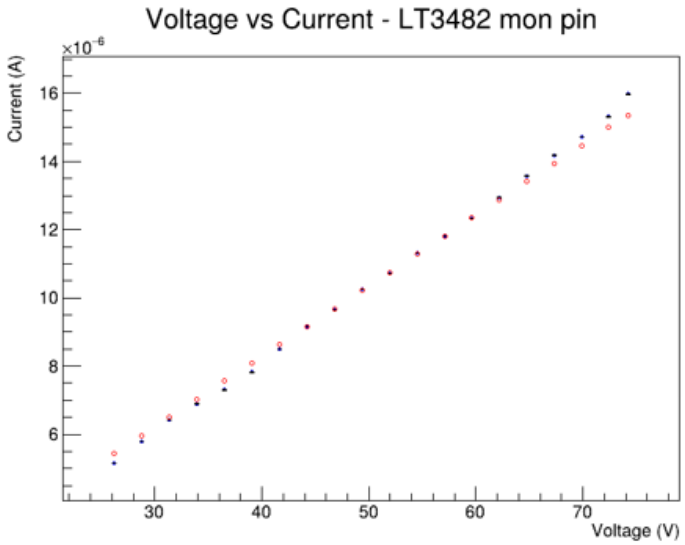

Figure 12: Measured current from the LT3482 monitor pin (scaled by the nominal factor of five) compared with the analytically calculated load cur- rent for a 4.3 MΩ resistor as a function of output voltage. The good agree- ment demonstrates that the MON pin provides a reliable and linear proxy for the SiPM current during operation.

the monitor output for continuous tracking of SiPM dark current and LED- induced signal current during calibration and long-term stability studies.

5.3 Measurements with Hamamatsu S13360-1350CS SiPM

The system was subsequently tested with a Hamamatsu series-13 SiPM, [13] S13360-1350CS, which has a nominal breakdown voltage of V_{BD} = 51.11 V. For the measurements presented here, the device was operated at an over- voltage of 5 V, corresponding to an applied bias voltage of approximately 56.1 V.

Low-intensity LED pulses were used to illuminate the device and generate resolvable multi-photoelectron charge spectra. Waveforms digitized by the DAQ system (Sec. 5.1) were integrated offline to form the charge distributions.

Both spectra exhibit clearly defined and regularly spaced photoelectron peaks, demonstrating excellent single-photon resolution at the chosen operating point. Depending on the illumination level, the spectra show identifiable peaks up to approximately N photoelectrons (to be updated after final analysis). The uniform peak spacing confirms the stability and linearity of the SiPM gain in the low-occupancy regime. No evidence of saturation or pulse pile-up is observed, indicating that the optical excitation and readout dynamic range are well matched to the measurement conditions.

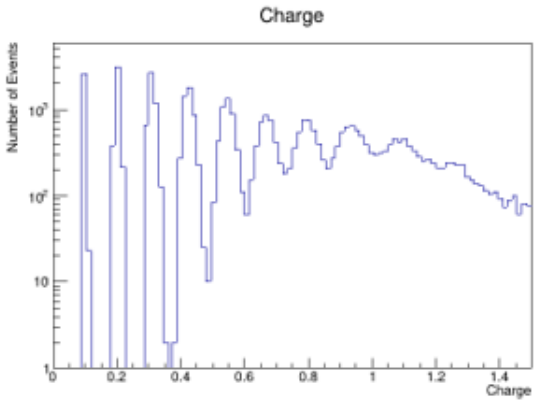

Figure 13: * (a) Low-light spectrum

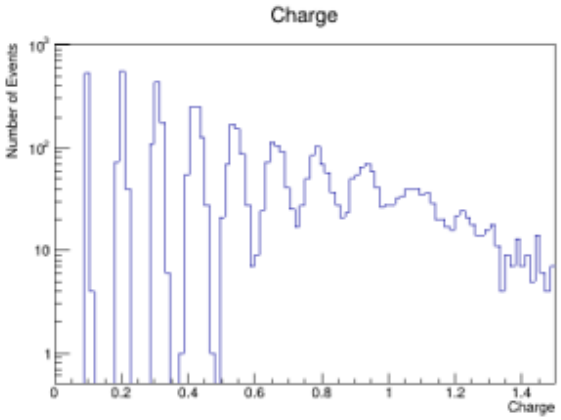

Figure 14: * (b) Higher-light spectrum

Figure 15: Charge spectra of the Hamamatsu S13360-1350CS SiPM oper- ated at 5 V overvoltage under two LED illumination settings. Multiple well-separated photoelectron peaks are visible, with the higher-intensity setting producing a larger number of resolvable peaks.

These measurements confirm that the LED calibration system, together with the custom bias supply and monitoring circuitry, provides stable and precise optical excitation suitable for SiPM gain calibration and long-term performance monitoring.

5.4 SiPM Current–Voltage Scan Using the Monitor Pin

In addition to monitoring the SiPM operating current, the LT3482 monitor pin (MON) was evaluated for approximate current–voltage characterization. The MON pin provides a current proportional to the load current, corresponding to 20% of the SiPM current, and can therefore be used to recon- struct the I–V dependence when the SiPM output is not directly accessible.

The SiPM bias voltage was scanned across the breakdown region while recording the monitor-pin current, corrected for the nominal scaling factor. The resulting I–V characteristic is shown in Fig. 16.

Although the monitor pin is primarily intended for operational current monitoring, these results show that it can also be used to estimate the SiPM breakdown voltage in constrained or sealed detector configurations. This method provides sufficient accuracy for operational monitoring, stability studies, and radiation-damage investigations, where relative shifts in breakdown voltage are of primary interest.

Cross-check Using Low-Side Current Measurement

As an independent cross-check, the SiPM breakdown voltage was also measured directly at the SiPM anode using the fully assembled bias and readout system. In this configuration, the SiPM current is measured via a low-side shunt resis tor using an INA228 precision current and power monitor, providing direct access to the absolute SiPM current independently of the LT3482 monitor pin.

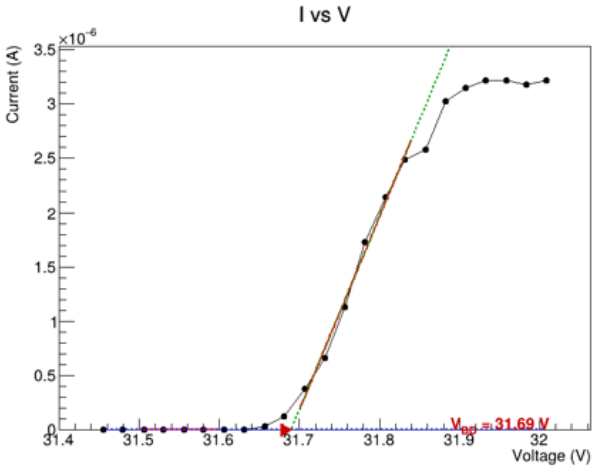

Figure 16: Current–voltage characteristic of the SiPM reconstructed from the LT3482 monitor pin during a bias voltage scan. The breakdown voltage, V_{BD} = 31.69 V, is obtained from the intersection of linear fits to the pre- breakdown and post-breakdown regions.

Figure 17 shows the SiPM current–voltage characteristic measured using the low-side shunt. The transition from the leakage region to the avalanche regime is clearly visible, in agreement with the I–V behavior reconstructed from the monitor pin.

To improve the precision of the breakdown voltage determination, the derivative of the logarithmic current with respect to voltage, $\mathrm{d}(\ln I)/\mathrm{d}V$, was computed from the measured I–V data. This method enhances sensitivity to the onset of avalanche multiplication and is commonly used for robust extraction of the SiPM breakdown voltage.

Figure 18 shows $\mathrm{d}(\ln I)/\mathrm{d}V$ as a function of bias voltage. The breakdown voltage is identified as the vol-

tage corresponding to the maximum of the derivative distribution.

The breakdown voltage values obtained using the low-side shunt measurement and the derivative method are consistent with those derived from the LT3482 monitor pin, confirming the validity of both approaches. This demonstrates that the proposed system allows reliable breakdown voltage monitoring using either embedded current monitoring or direct SiPM current sensing, depending on the accessibility and operational constraints of the detector configuration.

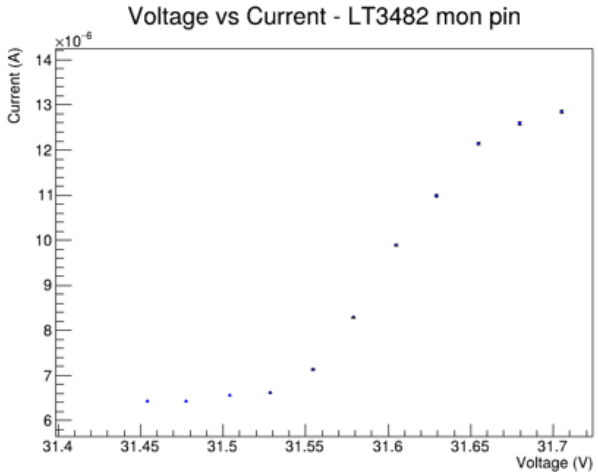

Figure 17: SiPM current–voltage characteristic measured directly at the SiPM anode using the INA228 current monitor on the low-side shunt resistor. The curve exhibits a clear transition at the breakdown voltage.

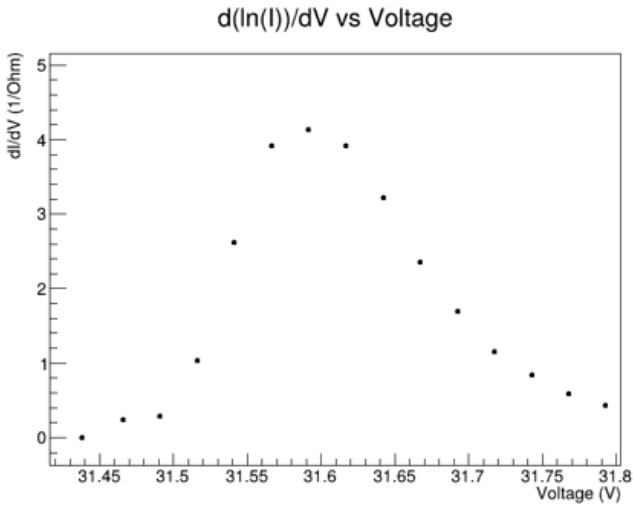

Figure 18: Derivative of the logarithmic SiPM current with respect to volt- age, d(ln *I*)/d *V*, obtained from the low-side current measurement. The peak position provides an alternative and precise estimate of the SiPM breakdown voltage.

Conclusion

A compact and flexible LED-based calibration system for silicon photomultiplier (SiPM) characterization has been developed and experimentally validated. The system integrates a digitally controlled multi-channel high- voltage power supply, a fast programmable LED pulser, and real-time current, voltage, and temperature monitoring within a unified control frame- work. This architecture enables precise and stable operation of SiPMs under controlled optical excitation, which is essential for gain calibration, break-down voltage determination, and long-term performance studies.

The LT3482-based high-voltage power supply demonstrated low noise, excellent voltage linearity, and reliable current monitoring through the in- tegrated monitor pin and external precision instrumentation. The DAC-controlled feedback scheme allows fine voltage adjustment and automated bias scans, making the system suitable for large-scale SiPM testing and characterization campaigns.

The LED excitation subsystem, combining a programmable DC bias with a fast MOSFET-based pulser, produced weak and well-defined optical pulses over a wide dynamic range. The fast pulser achieved sub-10 ns pulse widths with rise times below 4 ns, enabling precise synchronization with waveform acquisition and accurate reconstruction of single- and few- photoelectron spectra.

Temperature-dependent gain variations were addressed through continuous monitoring using PT100 sensors and constant-current excitation circuits. The implemented feedback mechanism provides real-time bias compensation, maintaining stable SiPM overvoltage under varying thermal conditions. This capability is particularly important for long-duration measurements and radiation damage studies where environmental stability cannot be guaranteed.

Experimental validation with Hamamatsu S13360 series SiPMs confirmed the system's ability to resolve individual photoelectron peaks with high sta- bility and reproducibility. Current–voltage scans using both the LT3482 monitor pin and low-side shunt measurements yielded consistent breakdown voltage determinations, demonstrating the versatility of the monitoring approach for both operational control and detector characterization.

Overall, the presented calibration platform offers a compact, modular, and cost-effective solution for comprehensive SiPM testing. Its scalability, digital control, and integrated monitoring make it well suited for laboratory characterization, quality assurance, and long-term performance studies, including investigations of radiation-induced degradation effects. Future developments may include expansion to a larger number of bias channels, integration of automated data analysis routines, and adaptation for insitu calibration of detector systems.

References

1. Querol, M., Rodríguez, J., Toledo, J., Esteve, R., Álvarez, V., & Herrero, V. (2016). A programmable, multichannel power supply for SiPMs with temperature compensation loop and Ethernet interface. *Journal of Instrumentation, 11*, C12035. https://doi.org/10.1088/1748-0221/11/12/C12035
2. Garutti, E., et al. (2011). Silicon photomultipliers for high energy physics detectors. *Journal of Instrumentation, 6*, C10003.
3. Analog Devices. (n.d.). *LT3482: High voltage bias controller* [Datasheet].
4. Texas Instruments. (n.d.). *DAC60504: 16-bit quad DAC* [Datasheet].
5. Texas Instruments. (n.d.). *INA228: Precision current and power monitor* [Datasheet].
6. Texas Instruments. (n.d.). *OPA452: High-voltage operational amplifier* [Datasheet].
7. Texas Instruments. (n.d.). *LM2596 SIMPLE SWITCHER power converter* [Datasheet].
8. Microchip Technology. (n.d.). *MCP4725: 12-bit DAC with I2C interface* [Datasheet].
9. Maxim Integrated. (n.d.). *DS1023 programmable delay line* [Datasheet].
10. Analog Devices. (n.d.). *LT1720 ultrafast comparator* [Datasheet].
11. Texas Instruments. (n.d.). *SN74AHC08 quad 2-input AND gate* [Datasheet].
12. Analog Devices. (n.d.). *LTspice XVII circuit simulation software*. https://www.analog.com/ltspice
13. Hamamatsu Photonics. (n.d.). *MPPC S13360 series* [Datasheet].
14. CAEN S.p.A. (n.d.). *V1720: 12-bit 250 MS/s waveform digitizer* [User manual/Datasheet].
15. CAEN S.p.A. (n.d.). *A4818: USB-to-optical link interface* [User manual/Datasheet].
16. ON Semiconductor. (n.d.). *J310 N-channel depletion-mode JFET* [Datasheet].
17. Keithley Instruments. (n.d.). *Model 2000 digital multimeter* [User manual/Datasheet].

UDC 539.1.074
SCOPUS CODE 3101
https://doi.org/10.36073/1512-0996-2026-2-175-191

SiPM-ის დახასიათებისთვის LED-ზე დაფუძნებული კალიბრაციის სისტემა

ალექსი მესტვირიშვილი საქართველოს ტექნიკური უნივერსიტეტის კვანტური ფიზიკისა და საინჟინრო ტექნოლოგიების ინსტიტუტის უფროსი მეცნიერი თანამშრომელი, საქართველო
E-mail: alexi.mestvirishvili@cern.ch

იური ბაღათურია საქართველოს ტექნიკური უნივერსიტეტის კვანტური ფიზიკისა და საინჟინრო ტექნოლოგიების ინსტიტუტის მთავარი მეცნიერი თანამშრომელი, საქართველო
E-mail: Iuri.bafaturia@cern.ch

ირაკლი ლომიძე საქართველოს ტექნიკური უნივერსიტეტის კვანტური ფიზიკისა და საინჟინრო ტექნოლოგიების ინსტიტუტის უფროსი მეცნიერი თანამშრომელი, საქართველო
E-mail: Irakli.lomidze@cern.ch

დავით ლომიძე საქართველოს ტექნიკური უნივერსიტეტის კვანტური ფიზიკისა და საინჟინრო ტექნოლოგიების ინსტიტუტის მეცნიერი თანამშრომელი, საქართველო
E-mail: David.lomidze@cern.ch

თენგიზ ტორიაშვილი საქართველოს ტექნიკური უნივერსიტეტის კვანტური ფიზიკისა და საინჟინრო ტექნოლოგიების ინსტიტუტის მეცნიერი თანამშრომელი, საქართველო
E-mail: Tengizi.toriashvili@cern.ch

აბესალომ იაშვილი საქართველოს ტექნიკური უნივერსიტეტის კვანტური ფიზიკისა და საინჟინრო ტექნოლოგიების ინსტიტუტის ინჟინერი, საქართველო
E-mail: iashviliab@yahoo.com

ზვიადი წამალაიძე საქართველოს ტექნიკური უნივერსიტეტის კვანტური ფიზიკისა და საინჟინრო ტექნოლოგიების ინსტიტუტის მთავარი მეცნიერი თანამშრომელი, საქართველო
E-mail: ZviadiTsamalaidze@cern.ch

რეცენზენტები:

ი. მინაშვილი, ბირთვული კვლევის გაერთიანებული ინსტიტუტი, დუბნა, უფროსი მეცნიერი თანამშრომელი
E-mail: Irakli.minashvili@cern.ch

დ. ჩოხელი, საქართველოს ტექნიკური უნივერსიტეტის, კვანტური ფიზიკისა და საინჟინრო ტექნოლოგიების ინსტიტუტის მთავარი მეცნიერი თანამშრომელი
E-mail: dchokhel@cern.ch

ანოტაცია. შექმნილია კომპაქტური, შუქდიოდზე დაფუძნებული დაკალიბრების სისტემა სილიციუმის ფოტოგამამრავლებლების (SiPM) კლასიფიკაციისა და დაკალიბრებისთვის. ასეთი დაკალიბრების სადგურები აუცილებელია SiPM-ების მახასიათებლების ზუსტი განსაზღვრისთვის, გარღვევის ძაბვის მონიტორინგისთვის და გრძელვადიანი სტაბილურობის კვლევებისთვის თანამედროვე ფოტოდეტექტორულ დანადგარებში. სისტემა აერთიანებს SiPM-ების ოთხარხიან კვების წყაროს, ციფრული ანალოგური გამყვანით კონტროლირებულ შუქდიოდზე დაფუძნებულ გარე სწრაფ პულსერს, რომელიც გვაძლევს მოკლე, პროგრამირებად ელექტრულ იმპულსებს. ნაშრომში აღწერილია სისტემის ძირითადი ბლოკები და მათი როლი დაბალი ინტენსივობის, კარგად განსაზღვრული ოპტიკური სიგნალების წარმოქმნაში, რომლებიც შესაფერისია ერთფოტონიანი და რამდენიმეფოტონიანი გაზომვებისთვის

საკვანძო სიტყვები: დაკალიბრების სადგურები; პულსები; სილიციუმის ფოტოგამმრავლებლები; ფოტოდეტეტორული დანადგარები.

The date of review 05.02.2026
The date of submission 12.02.2026
Signed for publishing 26.06.2026